DESIGN BIO-INSPIRED COMPOSITE STRUCTURE SUBJECTED TO BLAST LOADING

Phuong Tran[1,c], Abdallah Ghazlan[1,a], Tuan Ngo[1,b],
[1]Department of Infrastructure Engineering, The University of Melbourne, Melbourne, VIC, Australia
[a]ghazlana@ unimelb.edu.au, [b]dtngo@unimelb.edu.au, [c]phuong.tran@unimelb.edu.au

ABSTRACT

This paper investigates the behaviour of a bio-inspired finite element composite model (that mimics the structure of nacre, the inner layer of molluscan shells) under blast loading. Nacre, which has attracted the attention of researchers over the past few decades, comprises 95% aragonite, brittle voronoi-like polygonal tablets that are joined by an organic matrix and arranged in a brick and mortar type structure. The best attempt made thus far in mimicking such complex geometry involved rebuilding the tablet contours via optical imaging. This method, which practically copies the nacreous structure, offers no control over the geometry, making it difficult, if not impossible to eventually develop composites that mimic nacre. To this end, the finite element model developed herein was constructed using voronoi diagrams and geometric algorithms capable of automatically generating staggered layers of voronoi-like aluminium tablets bonded together by a vinylester adhesive layer. Many studies have led to the belief that the magnificent toughness of nacre is mainly attributed to the inter-platelet adhesive bonds. Results obtained from the finite element analysis show that this is indeed true, and it is imperative that the adhesive bond exhibits adequate toughness in order to be able to spread damage across the entire composite, thereby delaying localised failure.

KEYWORDS

Nacre, composite panel, blast loading, voronoi structure, bio-inspired structure.

INTRODUCTION

Biological materials, meta-materials, woven fabrics, nano-polymers, composite sandwich panels and many others have recently been investigated by structural research engineers because of their unmatched mechanical performance over traditional engineering materials (Tran 2014; Ghazlan 2015; Imbalzano 2015; Nguyen 2015; Yang 2015). Nacre, the inner layer of mollusc shells, stands out among them as the toughest, boasting a fracture toughness of up to 1240J/m^2 (Barthelat 2007). Specifically, the nacreous structure comprises 95% aragonite, in brittle ceramic tablets (or bricks), which are joined by an organic matrix (mortar) and arranged in a bricks and mortar type structure. In particular, the most striking attribute of nacre is its toughness, which is 3000 times greater than its bulk constituent (brittle aragonite).

Much effort has been devoted to characterising the mechanical behaviour of this magnificent organism in order to understand the mechanisms responsible for its superior toughness. In fact, many have observed that the nacreous tablets are not flat, and that diffusive sliding between the tablets is the key mechanism responsible for nacre's unmatched toughness (Ghazlan 2015). Specifically, when the organic matrix deforms in its plastic state, the aragonite tablets begin to slide on one another. Because the tablets are not flat, a hardening effect is activated through the interaction between their wavy surfaces. This has the effect of spreading the tablet sliding mechanism across the entire volume, thereby increasing the energy absorbing capacity of the system and delaying localised failure.

From this mechanism, one can intuitively deduce that the contact area between the tablets is an important parameter in the design of a nacre-mimicking composite system. To this end, Wei et al (2012) and Dutta et al (2013) developed analytical models of a rectangular unit cell cut out from the nacreous structure, to quantify the optimal overlapping length of nacre under planar static and dynamic tensile loading, respectively. By maximising the strain energy density of the unit cell and minimising the shear stress in the matrix, they we able to obtain optimal overlapping lengths that were similar to that found in nacre. Although these results give some insight into the nacre's toughening mechanisms, they are inconclusive when it comes to structural applications because transverse loading is the dominant imposed action. Furthermore, the simplified geometry of the unit cell is inaccurate when considering the complex nacreous tablet arrangement, as the tablets are arbitrarily shaped polygons.

Barthelat et al (2007) found that nacre exhibits a voronoi-like tablet architecture through optical imaging of a red abalone specimen. They reconstructed the tablet contours and input them into a numerical model. This method, which practically copies the structure of nacre offers no control over the geometry, which becomes infeasible in the development of a nacre-mimicking composite.

The objective of this research is to develop a finite element model of a multi-layered composite structure that mimics the geometric structure of nacre. The model will be applied to predict the performance of the composite under blast loading until catastrophic failure. In this work, we also develop geometric algorithms for generating the components in each layer of this composite structure, namely the polygonal nacreous voronoi tablets and the cohesive elements to bond them together.

FINITE ELEMENT MODEL

Construction of the nacre-mimicking geometry

Voronoi diagrams, which are well-known in computational geometry, are employed in this work to construct the geometry of the nacre-mimicking finite element model. Briefly, a voronoi diagram comprises of sites (or points) as shown in Figure 1, where every point inside the polygon enclosing the site is closest to that site. Mathematically, this can be represented by the following equation:

$$R_k = \{x \in X | d(x, P_k) \leq d(x, P_j) \forall j \neq k\}$$

Where R_k is the set of all points in the voronoi diagram X such that the distance $d(x, P_k)$ between each point x and a site P_k is less than or equal to the distance $d(x, P_j)$ between x and any other site P_j. The simplest possible configuration for a voronoi diagram is shown below in Figure 1a, where the sites are arranged in a grid to form square voronoi regions. By staggering the sites, the voronoi regions become hexagons (Figure 1b).

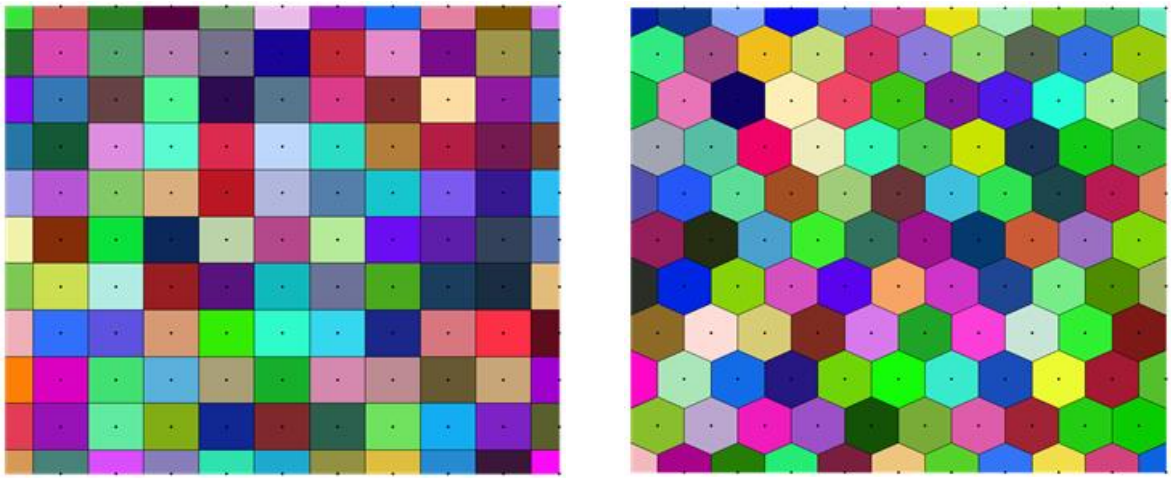

Figure 1 (a) Grid arrangement of voronoi sites yielding square voronoi regions; and (b) staggered arrangement of voronoi sites yielding hexagonal voronoi regions.

It can be observed from Figure 1 that the polygons at the boundary of the voronoi diagram are cut off. If this were not the case, they would extend infinitely, as the voronoi diagram has no boundary. To address this limitation, rectangular cropping is defined as an imaginary boundary, and the polygons are then cut to lie inside this region (Figure 2).

The abovementioned procedure was illustrated for a simple case, where the voronoi polygons are squares or hexagons. This can be extended to a more general case where the polygons become arbitrary regions as illustrated in Figure 3. The geometry of these regions can be manipulated by placing an imaginary circle around each site and allowing the site to move randomly within this circle according to equation 1, which dictates its position (x, y) in polar coordinates:

$$x = x_0 + rcos(\theta);\ y = y_0 + rsin(\theta) \quad (1)$$

Where: $(x_0 y_0)$ is the reference position of the site i.e. in a grid formation (Figure 1); r is a random value in the range $[0, R]$, where R is the chosen radius of the circle and; θ is a random angle in the range $[0, 2\pi]$. The radius R

is chosen as a function of the inter-layer overlapping area found in nacre, which is one-third of the area of the tablets on average. The resulting nacreous layer is shown in Figure 2a.

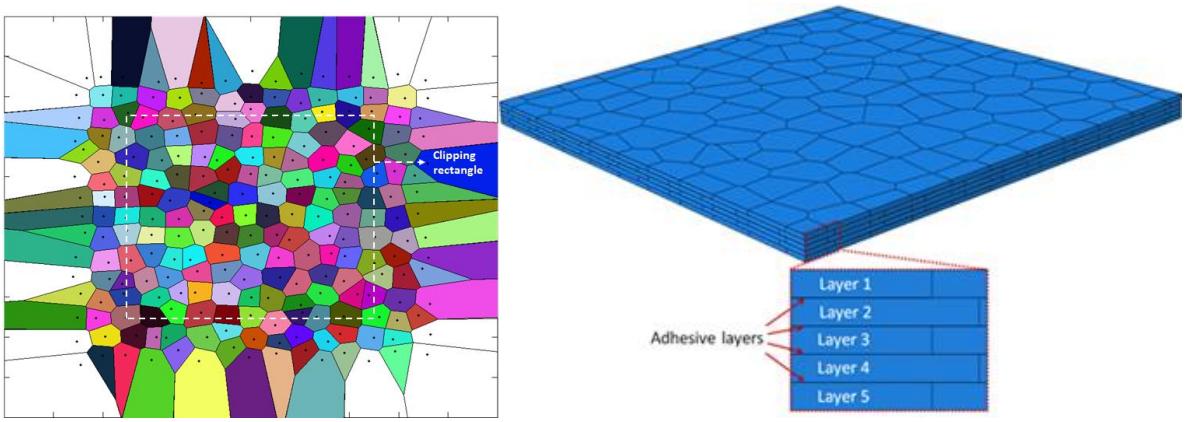

Figure 2 a) An example of a general voronoi diagram resembling a nacreous layer; and b) Assembled model mimicking nare's structural architecture, with nacreous layers bonded together by zero-thickness adhesive layers.

The next step involved the automatic insertion of zero-thickness cohesive elements between the grains of the platelets. To achieve this, the geometry of the nacreous layer illustrated in Figure 2a was imported into the finite element program ABAQUS and meshed. The mesh was then operated on directly to insert the cohesive elements between the voronoi polygons systematically. A simple example of this procedure is illustrated in Figure 3. Once the polygons were all connected by cohesive elements, they were extruded to form a three-dimensional nacrous layer. It is important to note that the node ordering required by the finite element (FE) program (ABAQUS in this case) is adhered to i.e. the stacked orientation of the cohesive elements is used to distinguish axial and shear behaviour. The above process is then repeated to generate five staggered layers, as illustrated by the brick and mortar arrangement in Figure 2b. The nacreous layers are then tied together by adhesive layers of negligible thickness, forming the composite model.

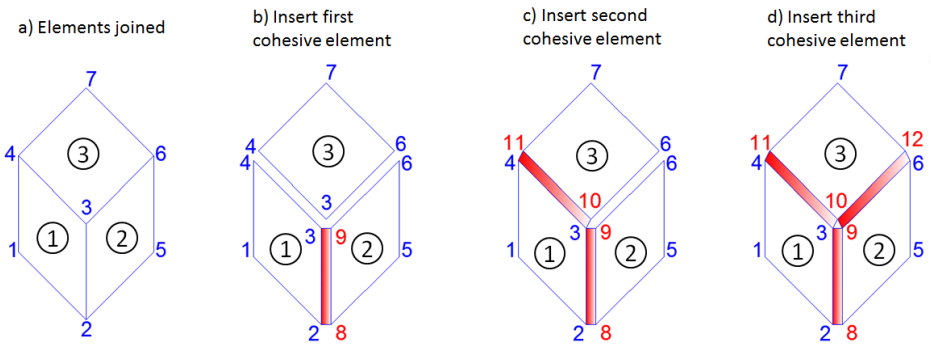

Figure 3 Simple process of cohesive element insertion at a junction formed by three elements.

MATERIAL MODEL

Cohesive model for composite interface

Delamination is an important failure mode in composite materials subjected to transverse loads. It can cause a significant reduction in the compressive load-carrying capacity of a structure. The debonding behaviour of the composite can be simulated by the Cohesive Zone Model (CZM).

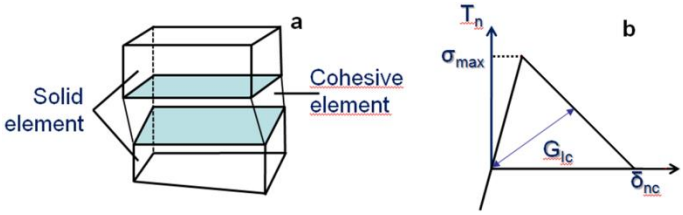

Figure 4 (a) 3D Eight-node cohesive element; (b) Rate-independent bilinear cohesive model.

This research employed a bilinear cohesive model illustrated in Figure 4b. The cohesive elements with finite thickness connect two volumetric elements as shown in Figure 4a with traction-separation laws, which relate the cohesive traction vectors T={t_n, t_s, t_t} and the displacement jump $\boldsymbol{\delta}$ ={δ_n, δ_s, δ_t}, where the subscripts n, s and t, respectively, denote the normal and tangential components. We adopt a simple bilinear cohesive law for damage initiation:

$$\left\{\frac{\boldsymbol{t_n}}{\boldsymbol{t_n^0}}\right\}^2 + \left\{\frac{\boldsymbol{t_s}}{\boldsymbol{t_s^0}}\right\}^2 + \left\{\frac{\boldsymbol{t_t}}{\boldsymbol{t_t^0}}\right\}^2 = \mathbf{1} \tag{2}$$

Where $\boldsymbol{t_n^0, t_s^0, t_t^0}$ represent the peak values of the nominal stress when the deformation is either purely normal to the interface, or purely in the first or the second shear direction, respectively. The power law form was adopted to describe the rate of stiffness degradation:

$$\left\{\frac{\boldsymbol{G_n}}{\boldsymbol{G_n^C}}\right\}^2 + \left\{\frac{\mathbf{G_s}}{\boldsymbol{G_s^C}}\right\}^2 + \left\{\frac{\mathbf{G_t}}{\boldsymbol{G_t^C}}\right\}^2 = \mathbf{1} \tag{3}$$

Where $\boldsymbol{G_n^C, G_s^C, G_t^C}$ refer to the fracture energy required to cause failure in the normal and shear directions, respectively. The cohesive material model adopted in this work is representative of vinylester resin and its properties are tabulated below.

Table 1 Vinylester cohesive material model

t_n^0, t_s^0, t_t^0	80 MPa
G_n^C, G_s^C, G_t^C	$1\,J/m^2$
ρ	$1850\,kg/m^3$
E_{nn}	4 GPa
E_{ss}, E_{tt}	1.5 GPa

- **Rate-dependent model for the nacreous tablets**

A rate-dependent material model was adopted to simulate the behaviour of the polygonal tablets. The Johnson-Cook constitutive law (for the Von Mises flow stress) for ductile metals (Johnson and Cook 1983) was utilised to predict this behaviour as follows:

$$\sigma = [A + B\epsilon^n][1 + Cln\dot{\epsilon}^*][1 - T^{*m}] \tag{4}$$

Where A represents the yield stress; $\boldsymbol{\epsilon}$ is the equivalent plastic strain; B and n account for the effects of strain hardening; $\dot{\boldsymbol{\epsilon}}^* = \dot{\boldsymbol{\epsilon}}/\dot{\boldsymbol{\epsilon}}_\mathbf{0}$ is the dimensionless strain rate for the reference strain rate $\dot{\boldsymbol{\epsilon}}_\mathbf{0} = \mathbf{0.001}\boldsymbol{s^{-1}}$; the constant C is obtained from experiment (tension, torsion, etc.); and the temperature $\boldsymbol{T^{*m}}$ is ignored, assuming isothermal conditions. The material employed in this work is Aluminium AA5083-H116, with properties listed in Table 2.

Table 2 Aluminium AA5083-H116 material model

ρ	$2750\ kg/m^3$
Elastic	
E	70 GPa
ν	0.3
Plastic	
A	215 MPa
B	280 MPa
n	0.404
m	0.859
C	0.0085
$\dot{\varepsilon}_0$	$0.001\ s^{-1}$

- **Blast model**

The Conventional Weapon Effects (CONWEP) card in ABAQUS was used to simulate blast loading on the front face of the nacreous composite, which is equivalent to a 0.15 kg TNT charge at a standoff distance of 0.5 m. The peak incident overpressure for this case is approximately 15 MPa, which is representative of a close range detonation.

RESULTS

Figure 5 illustrates the damage contours in the adhesive layer at the back face of the nacreous composite. Initation of damage occurred at t=1.2 ms, whilst the onset of failure occurred at t=1.5 ms. It can be observed that damage is nucleating and propagating out from the center of the adhesive layer until catastrophic failure occurs at t=2 ms. This is due to the low fracture toughness of the vinylester adhesive, which is two to three orders of magnitude smaller than that of nacre. Specifically, premature failure of the adhesive does not allow for the tablet sliding mechanism to be activated over the volume of the composite, leading to localised failure.

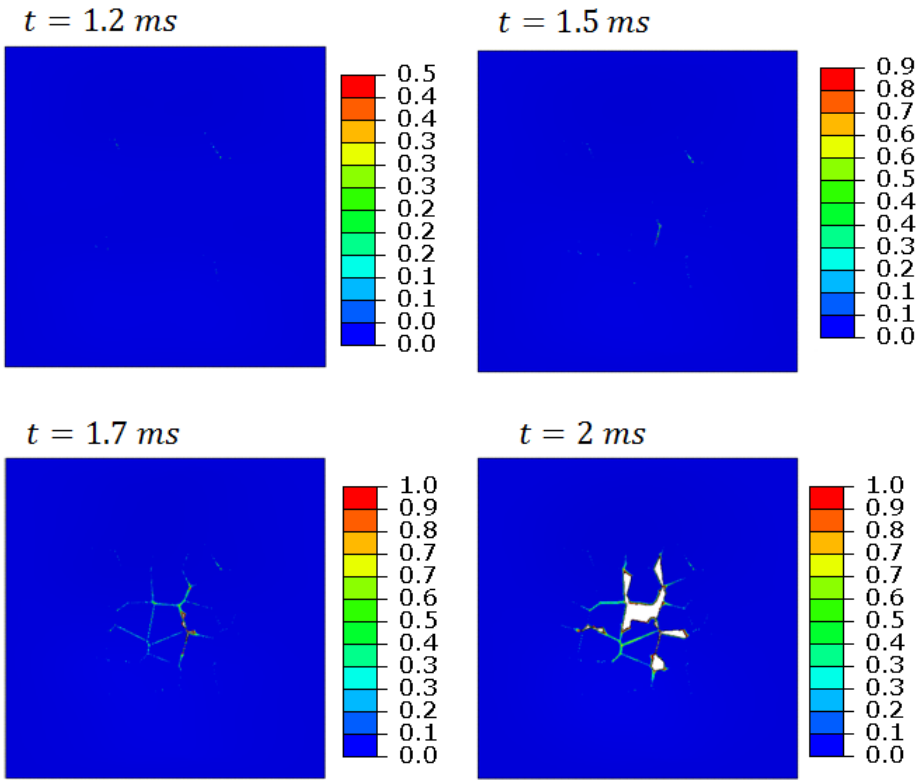

Figure 5 Damage contours in the adhesive layer near the back face of the nacreous composite.

The Von Mises stress distributions of a monolithic plate (of equal areal mass) are compared with the nacreous composite. The stress patterns are in close agreement between both models up to t=1.5 ms. This means that the

nacreous composite was able to spread out its deformation mechanism from the region of damage initiation since the stiffness of the adhesive layer did not degrade significantly. At the onset of failure (t=1.7 ms), the stiffness of the adhesive degrades entirely in the central region leading to stress concentrations in the tablets as there is no hardening mechanisms operating to delayed localised failure. This is evident in the increasing stress gradient observed from t=1.7 ms to t=2 ms in Figure 6 below.

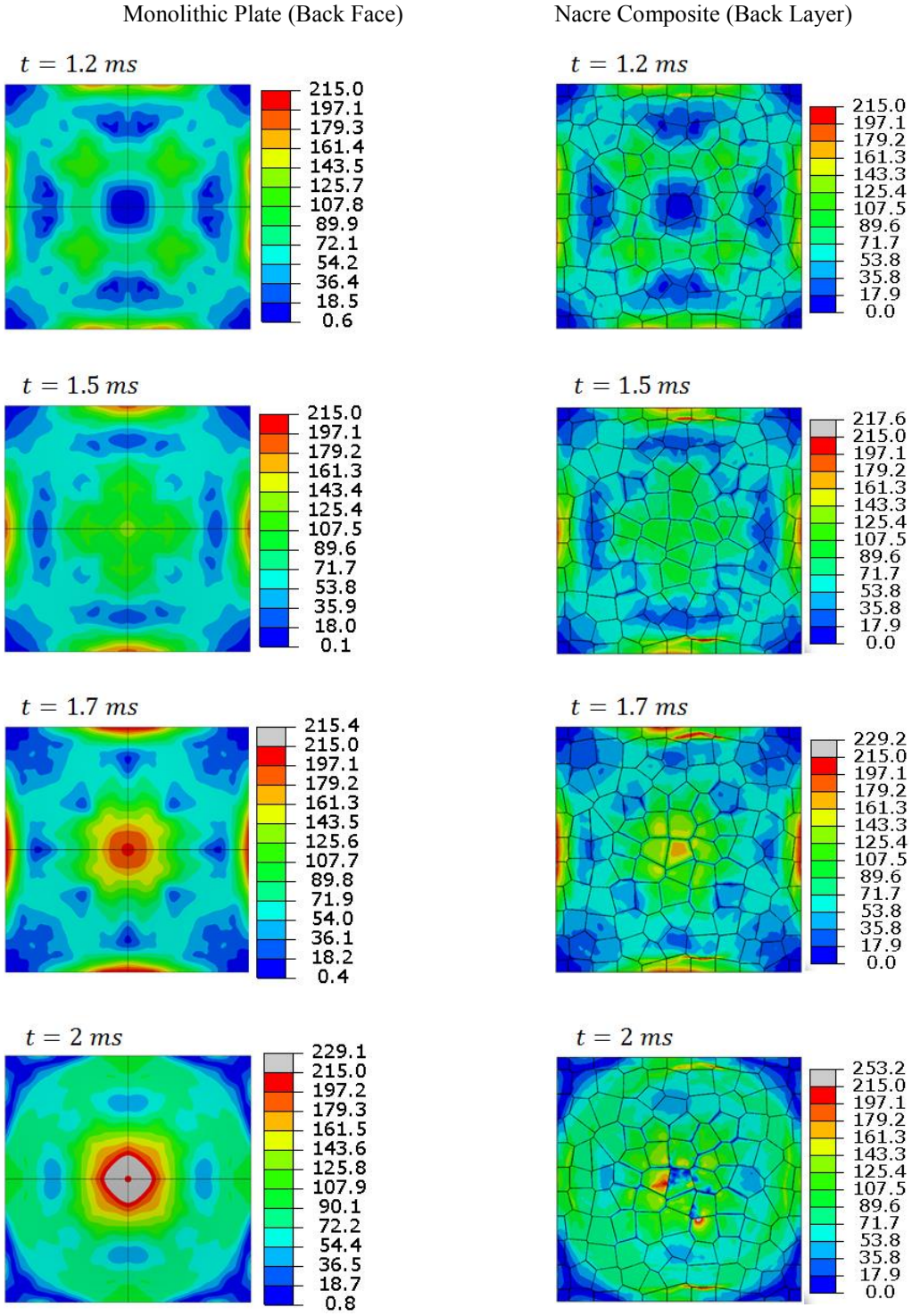

Figure 6 Von Mises stress comparison between the back face of the monolithic plate (left) and the back layer of the nacre composite (right). The cases where the damage initiated in the nacre composite (t=1.2 ms) to the runtime (t=2 ms) are shown. Both models are of equal areal mass

The plots for several components of energy are compared between the monolithic plate and the nacre composite in Figure 7. A close correlation between the kinetic and internal energies can be observed. The main mechanism of energy dissipation that operates in the nacre composite is damage. This is significant because a region of localised stress forms in the tablets, such that the plastic deformation mechanism is not spread out among the tablets (see Figure 6). This behaviour can be correlated to the minor plastic dissipation energy in both models observed in Figure 7. The monolithic plate dissipates a negligible amount of energy via plastic deformation, and no damage energy dissipation occurs at all. This is because the majority of the energy due to the blast load is absorbed by the monolithic plate in the form of recoverable strain energy.

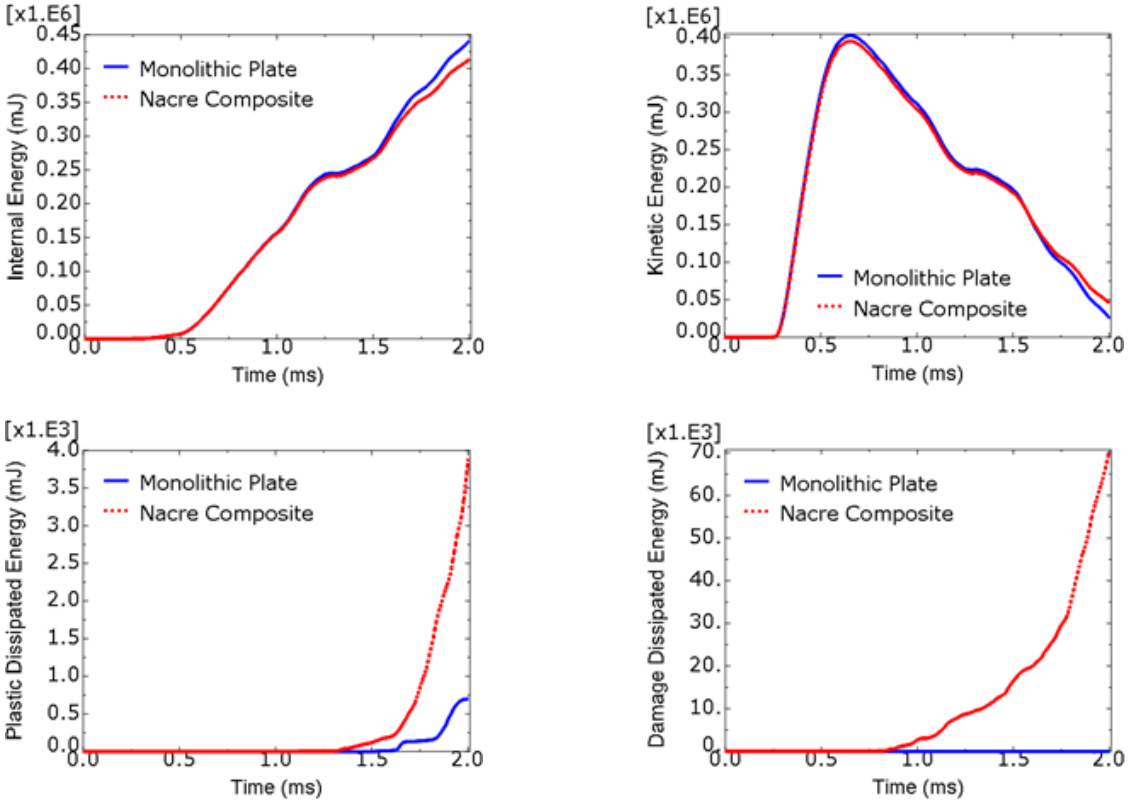

Figure 7 Energy comparisons between the monolithic plate and the nacre composite

The transverse displacements and velocities at the back face of the monolithic plate and the nacre composite are compared in Figure 8. A significant difference between the velocities of both models can be observed at the onset of failure (t=1.7 ms). The displacements between both models show close agreement. Contrary to the monolithic plate, the nacre composite cannot recover back to its equilibrium position due to localised failure of the adhesive. Therefore, the importance of the toughness of the adhesive layer cannot be overstated.

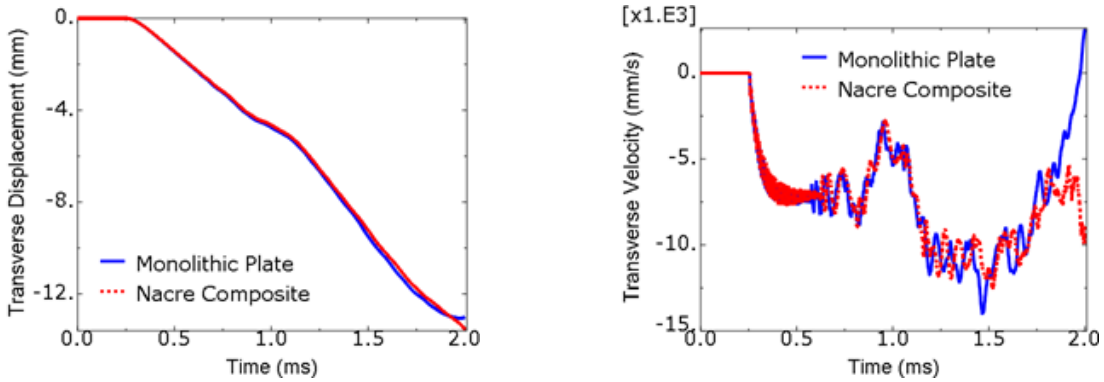

Figure 8 Transverse displacement (left) and velocity (right) comparisons between the monolithic plate and the nacre composite

CONCLUSION

A nacre-mimicking composite model was subjected to blast loading and its mechanical behaviour was compared to a monolithic plate of equal areal mass. Similar behaviour was observed between both models until the onset of failure, where the stiffness of the nacre composite degraded entirely. This is attributed to the low toughness of the adhesive material bonding the nacreous layers together, which leads to stress localisations that inhibit the spread of the deformation mechanism across the volume of the composite. Further research is required to verify this, and to investigate the influence of the interactions between the tablet surfaces of wavy geometries on the energy absorption capacity of the composite, by introducing additional toughness to the adhesive layer.

REFERENCES

Barthelat, F., H. Tang, and P. Zavattieri. (2007). "On the mechanics of mother-of-pearl: A key feature in the material hierarchichal structure". *Journal of the Mechanics and Physics of Solids*, 2007. **55**: p. 306-337.

Dutta, A., A. Tekalur, and M. Miklavcic. (2013). "Optimal overlap length in staggered architecture composites under dynamic loading conditions". *Journal of the Mechanics and Physics of Solids*, 2013. **61**.

Ghazlan, A., T. Ngo, and P. Tran. (2015). "Influence of interfacial geometry on the energy absorption capacity and load sharing mechanisms of nacreous composite shells". *Composite Structures*, 2015. **132**: p. 299-309.

Imbalzano, G., T. Ngo, and P. Tran. (2015). "A numerical study of auxetic composite panels under blast loadings". *Composite Structures*, 2015: p. Accepted 03 August 2015.

Johnson, G.R. and W.H. Cook. (1983). "A constitutive model and data for metals subjected to large strains, high strain rates and high temperatures". in *Proceedings of the 7th International Symposium on Ballistics*. 1983.

Nguyen, Q.T., T. Ngo, P.A. Tran, P. Mendis, and D. Bhattacharyya. (2015). "Influences of clay and manufacturing on fire resistance of organoclay/thermoset nanocomposites". *Composites Part A: Applied Science and Manufacturing*, 2015. **74**: p. 26-37.

Tran, P. and T. Ngo. (2014). "Bio-inspired composite structures subjected to underwater impulsive loading". *Computational Materials Science*, 2014.

Wei, X., M. Naraghi, and H.D. Espinosa. (2012). "Optimal length scales emerging from shear load transfer in natural materials: Application to carbon-based nanocomposite design". ACSNANO, 2012. **6**(3).

Yang, C.C., T. Ngo, and P. Tran. (2015). "Influences of weaving architectures on the impact resistance of multi-layer fabrics". *Materials and Design*, 2015. **85**(11): p. 282-295.